Arbitrary Power Sharing Among Three-Phase Winding Sets of Multiphase Machines

Ivan Zoric, *Student Member, IEEE,* Martin Jones, Emil Levi, *Fellow, IEEE*

Abstract–The paper develops a technique for arbitrary power sharing among three-phase winding sets of a multiphase generator. Multiple *d-q* modelling is commonly used when independent control of the winding sets is required. This work utilises instead the vector space decomposition modelling as the starting point and combines it with multiple *d-q* approach to preserve the advantages of the vector space decomposition, while still enabling independent control over each winding set. The power sharing is achieved by imposing appropriate *x-y* currents at the fundamental frequency, so that flux and average torque are not affected. The theory is developed initially for the nine-phase machine. A general expression for arbitrary current sharing is derived further for any multiphase machine with multiple three-phase windings. The obtained equations are valid for any possible machine topology (asymmetrical/ symmetrical, with single or multiple neutral points). The theory is validated experimentally using an asymmetrical nine-phase induction generator with indirect rotor field oriented control.

Index Terms–Induction motors, Machine vector control, Multiphase drives, Power sharing, Pulse width modulation converters, Variable speed drives, Wind energy generation.

NOMENCLATURE

$i_{a,b,c,d,e,f,g,h,i}$, i_{phase}	Stator phase currents.
$i_{aj,bj,cj}$	j^{th} winding set stator phase currents.
$i_{d,q}$	VSD d-q stator current components in a rotating reference frame.
$i_{dj,qj}$	j^{th} stator winding set d-q currents.
$i_{dxyj,qxyj}$	VSD x_j-y_j subspace current components in a rotating reference frame.
I_n	Rated RMS phase current.
i_{VSD}	VSD stator current component matrix.
$i_{\alpha,\beta}$, $i_{xj,yj}$	VSD α-β and x_j-y_j current components.
i_z, i_{zj}	Single and j^{th} winding set neutral point current.
$i_{\alpha j,\beta j}$, $I_{\alpha\beta j}$, $\varphi_{\alpha\beta j}$	j^{th} winding set α-β currents, space vector amplitude and angle.

$I_{\alpha\beta}$, $\varphi_{\alpha\beta}$, I_{xyj}, φ_{xyj}	VSD α-β and x_j-y_j subspace current space vector amplitude and angle.
k_i	Current sharing coefficient of the ith winding set.
L_{ls}, L_{lr}	Stator and rotor leakage inductance.
L_s, L_m, L_r	Stator, mutual and rotor inductance.
R_s, R_r	Stator and rotor resistance.
P_{el}	Machine's electrical power.
P_{wsj}	j^{th} winding set electrical power.
$[T_3]$	3-phase Clarke's transformation matrix.
$[T_{9a1}]$, $[T_{9a3}]$	Asymmetrical 9-phase VSD matrices, one and three neutral points.
$[T_{9s1}]$, $[T_{9s3}]$	Symmetrical 9-phase VSD matrices, one and three neutral points.
α	Winding set propagation angle.
T_m, T^*	Measured torque and torque reference.
v	Voltages – come with the same indices as currents in various subspaces.
ψ^*_{dr}	Rotor flux reference.
θ_{el}	Rotor flux angular position.
$[\theta_a]$, $[\theta_s]$	Symmetrical and asymmetrical 9-phase machine phase propagation angles.
ω_e, ω_m	Rotor electrical and mechanical speed.
P, ω_{el}	Pole pair number, rotor flux speed.
$*$	Superscript - reference value.
$\_$	Underlining denotes space vectors.
r	Index – rotor variables and parameters.

I. INTRODUCTION

Use of wind energy conversion systems (WECS) is increasing and the world annual growth in wind power production in 2015 was 63 GW. The total installed power reached 433 GW [1] and the size of the wind turbines has also increased. The power of multi-MW wind turbines has reached 8 MW [2-4]. Although the majority of WECS use three-phase machines [4], there is a growing interest in using multiphase machines [5-10]. When compared to the three-phase equivalents, multiphase machines have lower current/power per phase, lower torque ripple and above all are inherently fault tolerant [11-13]. These advantages make them well suited for remote offshore wind farms. The dominant multiphase stator design is the one with distributed windings, which produces near-sinusoidal flux distribution. This machine type is considered in this paper.

1

The stator phase number of a multiphase machine may be a prime number or a composite number (use of multiple winding sets). Moreover, if the winding sets are three-phase ones, then the said machine is a multiple three-phase machine. This type is particularly attractive since standard three-phase inverters can be used to supply the machine. A noticeable increase in research undertaken for this particular type of multiphase machine has been reported recently [14-16]. The machine can be modelled by applying the well-known three-phase Clarke's transformation to each three-phase winding set [17, 18], followed by the standard three-phase rotational transformation. By doing so, the machine is divided into multiple flux/torque producing subspaces and well-known control techniques developed for three-phase machines can be implemented in each subspace [19]. The advantage of this modelling approach is the possibility for individual and independent control of all winding sets; hence, power/current sharing between winding sets is easily achieved. On the other hand, this multiple *d-q* modelling approach leads to heavy cross-coupling between equations of the different three-phase winding sets [20] and it also does not offer clear insight into machine operation and harmonic mapping. In addition, multiple pairs of PI controllers are required for flux/torque control.

Another approach to machine modelling is by use of the vector space decomposition (VSD) [21]. Vector space can be decomposed using multiphase complex or real (Clarke's) transformation matrices. The latter approach, as in [21, 22], is used throughout this paper. Depending on the machine type (symmetrical or asymmetrical), different ways of obtaining a VSD matrix have been devised [21-25]. This method decouples the machine into orthogonal subspaces: a single flux/torque producing (*α-β*) subspace and multiple non-flux/torque producing (*x-y*) subspaces. Rotational transformation is now applied to only the first (*α-β*) subspace, so that a single pair of current controllers enables full flux/torque control. Low-order harmonics and unbalance in phase variables map into the *x-y* subspaces and can be independently controlled [26-29]. However, information about the currents in individual winding sets is lost.

Multiple *d-q* modelling approach has been utilised in [30] to develop arbitrary power sharing between winding sets of an asymmetrical 12-phase machine. Although this is successfully achieved, heavy cross-coupling between equations of each winding set exists due to the used modelling approach. Power sharing using VSD approach has been discussed in [31-33]. In [31, 32] the sharing is examined for an asymmetrical 12-phase machine with four neutral points. Further, [33] implicitly uses power sharing between winding sets in order to balance individual dc link voltages in a six-phase machine with series-connected three-phase inverters. A different power sharing technique is developed by introducing a novel transformation matrix in [34], where auxiliary subspaces provide insight into currents of individual winding sets.

The aim of this paper is to combine both VSD and multiple *d-q* modelling approaches in order to preserve the benefits of the VSD approach while still being able to ascertain information about phase currents in individual winding sets. It is shown that the differences in these currents are manifested through *x-y* currents at fundamental frequency. Hence, current control in *x-y* planes enables arbitrary power/current sharing between winding sets, a desirable feature in a multiphase generator. The work reported in [31, 32] for an asymmetrical 12-phase machine is taken here further by considering a general case of a multiphase machine with multiple three-phase windings in both symmetrical and asymmetrical configurations, with both single and multiple neutral points.

While an asymmetrical six-phase machine topology is still widely considered in recent works [7, 8, 10, 26, 27, 33], there has been a substantial increase in the interest in the solutions with three [5, 9, 19, 22, 25, 34] and to a somewhat lesser extent four [9, 30-32] three-phase windings in the last ten years. Hence, power sharing between winding sets is developed first here for an asymmetrical nine-phase machine. It is shown that use of an appropriate VSD matrix provides the set of equations that are valid for all machine topologies (symmetrical/asymmetrical with single/three neutral points). Next, the approach is extended to any multiphase machine with multiple three-phase windings, irrespective of the topology and a set of equations that can be used in a general case is presented. The main contributions of this paper are:

- By combining the VSD and multiple *d-q* modelling approaches, correlation between individual winding set currents and currents in the VSD subspaces is found for a nine-phase machine. It is shown that when appropriate VSD transformation is used, the same set of equations is valid for all four topologies of a nine-phase machine. This enables decoupled control of the machine in VSD planes, with ability to control individual winding set powers.

- Based on the VSD transformation and multiple three-phase Clarke's transformation, equations enabling arbitrary control of individual three-phase winding set currents in a general case of a machine with *l* three-phase winding sets are developed using the VSD *x-y* planes. The equations are obtained by only combining transformation matrices; results are thus independent of the machine type (i.e. induction or synchronous).

- Obtained equations are used to develop a power sharing technique, while total flux and average torque production is unaffected.

- Numerical and experimental verification is provided. Experiments are conducted with an asymmetrical nine-phase induction machine with three neutral points. It is shown that developed power/current sharing technique does not have any effect on the total flux/torque control.

Potential applications of the devised power sharing algorithm depend on the actual WECS topology used and on whether the WECS supplies isolated loads or connects to the grid. In topologies where the WECS supplies the grid using parallel machine-side converters and either a single or multiple grid-side converters (Fig. 1a and Fig. 1c), the power sharing can be used in fault-tolerant mode when a whole three-phase machine-side converter is taken out of service due to, say, an open-circuit fault. If the WECS is realised with

series-connected dc links, as in Fig. 1b, then the power sharing enables balancing of the dc voltages of individual cascaded dc links. Last but not least, a WECS may be used to supply stand-alone loads, as illustrated in Fig. 1d and Fig. 1e. The loads can be ac micro-grids (or stand-alone ac loads), as assumed in Fig. 1d, or dc micro-grids, in which case there are only machine-side converters and dc micro-grids connect directly to the dc links (Fig. 1e). In the last two cases the power sharing can effectively satisfy potentially rather different power needs of the individual ac or dc micro-grids.

II. NINE-PHASE MACHINE MODELLING

An asymmetrical nine-phase induction machine with three isolated neutral points is considered first. The phase propagation angles of this machine are:

$$[\theta_a] = \begin{bmatrix} 0 & \dfrac{\pi}{9} & \dfrac{2\pi}{9} & \dfrac{6\pi}{9} & \dfrac{7\pi}{9} & \dfrac{8\pi}{9} & \dfrac{12\pi}{9} & \dfrac{13\pi}{9} & \dfrac{14\pi}{9} \end{bmatrix} \quad (1)$$

The phases are denoted by letters a, b, c, …, i; at the same time phases in each of the three-phase winding sets are denoted by a_j, b_j, c_j where index j represents winding set number. Magnetic axes and notation are shown in Fig. 2.
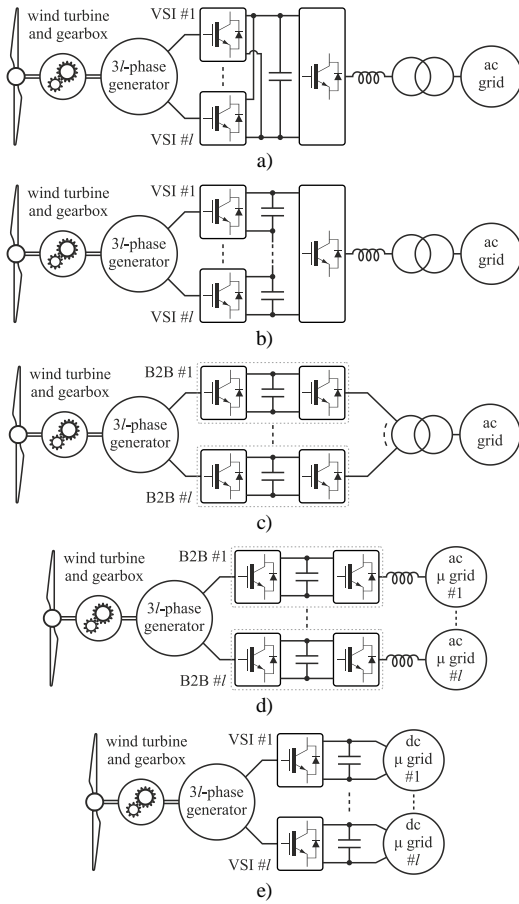

Fig. 1. WECS structures where generators with multiple three-phase windings are used in different topologies and for different loads: a) Parallel machine-side converter configuration, b) Cascaded dc link configuration, c) Back-to-back VSIs connected to the grid, d) Individual three-phase winding sets supplying individual isolated ac loads (μ grid = micro-grid), e) As d), but the stand-alone loads are dc micro-grids.

To decouple the machine into flux/torque producing (α-β plane) and non-flux/torque producing components (x-y planes and zero sequences), the following amplitude invariant VSD transformation [25] is used:

$$[T_{9a3}] = \frac{2}{9} \begin{bmatrix} \cos([\theta_a]) \\ \sin([\theta_a]) \\ \cos(5[\theta_a]) \\ \sin(5[\theta_a]) \\ \cos(7[\theta_a]) \\ \sin(7[\theta_a]) \\ \frac{3}{2}\ 0\ 0\ \frac{3}{2}\ 0\ 0\ \frac{3}{2}\ 0\ 0 \\ 0\ \frac{3}{2}\ 0\ 0\ \frac{3}{2}\ 0\ 0\ \frac{3}{2}\ 0 \\ 0\ 0\ \frac{3}{2}\ 0\ 0\ \frac{3}{2}\ 0\ 0\ \frac{3}{2} \end{bmatrix} \quad (2)$$

Subspaces in (2) are ordered to accommodate the derivation that follows. Assuming near-sinusoidal magneto-motive force distribution, induction machine equations are:

$$\begin{bmatrix} v_\alpha \\ v_\beta \\ 0 \\ 0 \end{bmatrix} = \begin{bmatrix} R_s + L_s\dfrac{d}{dt} & 0 & L_m\dfrac{d}{dt} & 0 \\ 0 & R_s + L_s\dfrac{d}{dt} & 0 & L_m\dfrac{d}{dt} \\ L_m\dfrac{d}{dt} & \omega_e L_m & R_r + L_r\dfrac{d}{dt} & \omega_e L_r \\ -\omega_e L_m & L_m\dfrac{d}{dt} & -\omega_e L_r & R_r + L_r\dfrac{d}{dt} \end{bmatrix} \begin{bmatrix} i_\alpha \\ i_\beta \\ i_{r\alpha} \\ i_{r\beta} \end{bmatrix} \quad (3a)$$

$$\begin{bmatrix} v_{xj} \\ v_{yj} \end{bmatrix} = \begin{bmatrix} R_s + L_{ls}\dfrac{d}{dt} & 0 \\ 0 & R_s + L_{ls}\dfrac{d}{dt} \end{bmatrix} \begin{bmatrix} i_{xj} \\ i_{yj} \end{bmatrix}, \quad j = 1, 2 \quad (3b)$$

$$v_{zj} = \left(R_s + L_{ls}\dfrac{d}{dt} \right) i_{zj}, \quad j = 1, 2, 3$$

where rotor equations have been transformed into the stationary reference frame. In order to obtain control of individual winding sets, the relation between VSD currents and currents of each winding set must be determined. Therefore, the following three-phase power-variant Clarke's transformation is used for the three three-phase windings:

$$[T_3(\alpha)] = \frac{2}{3} \begin{bmatrix} \cos(\alpha) & \cos\left(\alpha + \dfrac{2\pi}{3}\right) & \cos\left(\alpha + \dfrac{4\pi}{3}\right) \\ \sin(\alpha) & \sin\left(\alpha + \dfrac{2\pi}{3}\right) & \sin\left(\alpha + \dfrac{4\pi}{3}\right) \\ \dfrac{1}{2} & \dfrac{1}{2} & \dfrac{1}{2} \end{bmatrix} \quad (4)$$

where α takes values 0, π/9, and 2π/9, respectively. Application of (4) to phase currents results in three sets of α-β-z currents, one for each winding set.

Since VSD transformation provides correlation between phase and VSD variables, finding mapping of triple α-β-z currents into VSD subspaces requires definition of phase currents and their relationship with multiple α-β-z currents. Using Fig. 2, this relationship is governed with:

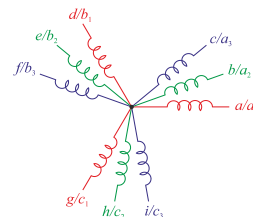

Fig. 2. Phase magnetic axes in an asymmetrical nine-phase machine.

$$\begin{bmatrix} i_a \\ i_d \\ i_g \end{bmatrix} = \begin{bmatrix} i_{a1} \\ i_{b1} \\ i_{c1} \end{bmatrix} = \left[T_3(0) \right]^{-1} \times \begin{bmatrix} i_{\alpha 1} \\ i_{\beta 1} \\ i_{z1} \end{bmatrix}$$

$$\begin{bmatrix} i_b \\ i_e \\ i_h \end{bmatrix} = \begin{bmatrix} i_{a2} \\ i_{b2} \\ i_{c2} \end{bmatrix} = \left[T_3\left(\frac{\pi}{9}\right) \right]^{-1} \times \begin{bmatrix} i_{\alpha 2} \\ i_{\beta 2} \\ i_{z2} \end{bmatrix} \qquad (5)$$

$$\begin{bmatrix} i_c \\ i_f \\ i_i \end{bmatrix} = \begin{bmatrix} i_{a3} \\ i_{b3} \\ i_{c3} \end{bmatrix} = \left[T_3\left(\frac{2\pi}{9}\right) \right]^{-1} \times \begin{bmatrix} i_{\alpha 3} \\ i_{\beta 3} \\ i_{z3} \end{bmatrix}$$

When phase currents (5) are arranged in a column vector $[i_a \ i_b, \dots, i_i]^T$ and multiplied by the VSD matrix (2), correlation between individual winding set α-β-z currents and VSD subspace currents is defined as:

$$\begin{bmatrix} i_\alpha \\ i_\beta \\ i_{x1} \\ i_{y1} \\ i_{x2} \\ i_{y2} \\ i_{z1} \\ i_{z2} \\ i_{z3} \end{bmatrix} = \left[T_{9a3} \right] \times \begin{bmatrix} i_a \\ i_b \\ i_c \\ i_d \\ i_e \\ i_f \\ i_g \\ i_h \\ i_i \end{bmatrix} \begin{bmatrix} \frac{1}{3}\left(i_{\alpha 1} + i_{\alpha 2} + i_{\alpha 3}\right) \\ \frac{1}{3}\left(i_{\beta 1} + i_{\beta 2} + i_{\beta 3}\right) \\ \frac{1}{6}\left(2i_{\alpha 1} - i_{\alpha 2} - i_{\alpha 3} + \sqrt{3}i_{\beta 2} - \sqrt{3}i_{\beta 3}\right) \\ \frac{1}{6}\left(\sqrt{3}i_{\alpha 2} - \sqrt{3}i_{\alpha 3} - 2i_{\beta 1} + i_{\beta 2} + i_{\beta 3}\right) \\ \frac{1}{6}\left(2i_{\alpha 1} - i_{\alpha 2} - i_{\alpha 3} - \sqrt{3}i_{\beta 2} + \sqrt{3}i_{\beta 3}\right) \\ \frac{1}{6}\left(\sqrt{3}i_{\alpha 2} - \sqrt{3}i_{\alpha 3} + 2i_{\beta 1} - i_{\beta 2} - i_{\beta 3}\right) \\ i_{z1} \\ i_{z2} \\ i_{z3} \end{bmatrix} \qquad (6)$$

Complex notation is used to give (6) in a compact form:

$$\underline{i}_{\alpha\beta} = i_\alpha + j i_\beta = I_{\alpha\beta} e^{j\varphi_{\alpha\beta}}$$

$$\underline{i}_{xy(1,2)} = i_{x(1,2)} + j i_{y(1,2)} = I_{xy(1,2)} e^{j\varphi_{xy(1,2)}} \qquad (7)$$

$$\underline{i}_{\alpha\beta(1,2,3)} = i_{\alpha(1,2,3)} + j i_{\beta(1,2,3)} = I_{\alpha\beta(1,2,3)} e^{j\varphi_{\alpha\beta(1,2,3)}}$$

resulting in:

$$\underline{i}_{\alpha\beta} = \frac{1}{3}\left(I_{\alpha\beta 1} e^{j\varphi_{\alpha\beta 1}} + I_{\alpha\beta 2} e^{j\varphi_{\alpha\beta 2}} + I_{\alpha\beta 3} e^{j\varphi_{\alpha\beta 3}} \right)$$

$$\underline{i}_{xy1} = \frac{1}{3}\left(I_{\alpha\beta 1} e^{-j\varphi_{\alpha\beta 1}} + I_{\alpha\beta 2} e^{-j\varphi_{\alpha\beta 2}} e^{j2\pi/3} + I_{\alpha\beta 3} e^{-j\varphi_{\alpha\beta 3}} e^{-j2\pi/3} \right) \qquad (8)$$

$$\underline{i}_{xy2} = \frac{1}{3}\left(I_{\alpha\beta 1} e^{j\varphi_{\alpha\beta 1}} + I_{\alpha\beta 2} e^{j\varphi_{\alpha\beta 2}} e^{j2\pi/3} + I_{\alpha\beta 3} e^{j\varphi_{\alpha\beta 3}} e^{-j2\pi/3} \right)$$

Zero-sequence equations are omitted further on, since three isolated neutral points are assumed.

Equations (6) and (8) provide correlation between currents of individual winding sets ($\underline{i}_{\alpha\beta(1,2,3)}$) that govern power drawn/supplied by the winding and currents in terms of VSD variables ($\underline{i}_{\alpha\beta}$, $\underline{i}_{xy(1,2)}$). Hence, they provide references for the x-y currents in order to achieve arbitrary control of power production in each of the winding sets. The first equation of (8) specifies an obvious constraint, that one third of a sum of $\underline{i}_{\alpha\beta(1,2,3)}$ currents is equal to the total flux/torque producing current $\underline{i}_{\alpha\beta}$. Accordingly, currents in two winding sets can be arbitrarily controlled while the third is constrained by the total flux/torque requirements.

From the first equation of (8), it follows that if all $\underline{i}_{\alpha\beta(1,2,3)}$ currents are aligned along the same axis, their amplitudes will be minimal (Fig. 3). Consequently, resistive losses are kept at the smallest possible value for any given degree of imbalance in power distribution (absolute minimal resistive losses result,

of course, with balanced power sharing). On the other hand, by applying the constraint for minimal resistive losses, angles $\varphi_{\alpha\beta}$ and $\varphi_{\alpha\beta(1,2,3)}$ are equal; hence arbitrary control of active and reactive power in individual winding sets is lost and one can control arbitrarily apparent powers only. This is of no relevance if the machine is a surface mounted permanent magnet synchronous one, since it is normally operated with zero reference for the flux producing current, but is relevant in the case of an induction machine. Although this problem can be circumvented, this is beyond the scope of this paper. Hence, current sharing coefficients are now defined as:

$$I_{\alpha\beta 1} = k_1 I_{\alpha\beta} \qquad I_{\alpha\beta 2} = k_2 I_{\alpha\beta} \qquad I_{\alpha\beta 3} = k_3 I_{\alpha\beta} \qquad (9)$$

Since amplitude invariant transformations (2) and (4) are used, current amplitudes ($I_{\alpha\beta 1}$, $I_{\alpha\beta 2}$, $I_{\alpha\beta 3}$) correspond to the phase current amplitudes. Therefore, current sharing coefficients (9) directly affect phase current amplitude in each of the winding sets. Subspace currents are then as follows:

$$\underline{i}_{\alpha\beta} = \frac{1}{3}(k_1 + k_2 + k_3) I_{\alpha\beta} e^{j\varphi_{\alpha\beta}}$$

$$\underline{i}_{xy1} = \frac{1}{3}\left(k_1 + k_2 e^{j2\pi/3} + k_3 e^{-j2\pi/3}\right) I_{\alpha\beta} e^{-j\varphi_{\alpha\beta}} \qquad (10)$$

$$\underline{i}_{xy2} = \frac{1}{3}\left(k_1 + k_2 e^{j2\pi/3} + k_3 e^{-j2\pi/3}\right) I_{\alpha\beta} e^{j\varphi_{\alpha\beta}}$$

It follows that x-y currents depend only on α-β currents and current sharing coefficients $k_{1,2,3}$. Since flux/torque control is usually implemented in a synchronous reference frame, equations (10) should be expressed using d-q currents. Hence, rotational transformation is applied to the 1st and the 3rd equation of (10) and inverse rotational transformation to the 2nd equation, using angles $\varphi_{\alpha\beta}$ and $-\varphi_{\alpha\beta}$, respectively. Equations for subspace currents become:

$$\underline{i}_{dq} = \frac{1}{3}(k_1 + k_2 + k_3) \underline{i}_{dq}$$

$$\underline{i}_{dqxy1} = \frac{1}{3}\left(k_1 + k_2 e^{j2\pi/3} + k_3 e^{-j2\pi/3}\right) \overline{\underline{i}}_{dq} \qquad (11)$$

$$\underline{i}_{dqxy2} = \frac{1}{3}\left(k_1 + k_2 e^{j2\pi/3} + k_3 e^{-j2\pi/3}\right) \underline{i}_{dq}$$

Dash above d-q current in the second equation indicates complex conjugate. The first equation of (10) and (11) sets the constraint that the sum of the current sharing coefficients $k_{1,2,3}$ should always be equal to three. If this is respected, the first equations of (10) and (11) can be omitted from further analysis. Finally, when equations (11) are returned to scalar form, references for x-y currents are given with:

$$\begin{bmatrix} i_{dxy1}^* \\ i_{qxy1}^* \end{bmatrix} = \frac{1}{6} \begin{bmatrix} (2k_1 - k_2 - k_3) & \sqrt{3}(k_2 - k_3) \\ \sqrt{3}(k_2 - k_3) & -(2k_1 - k_2 - k_3) \end{bmatrix} \begin{bmatrix} i_d \\ i_q \end{bmatrix}$$

$$\begin{bmatrix} i_{dxy2}^* \\ i_{qxy2}^* \end{bmatrix} = \frac{1}{6} \begin{bmatrix} (2k_1 - k_2 - k_3) & -\sqrt{3}(k_2 - k_3) \\ \sqrt{3}(k_2 - k_3) & (2k_1 - k_2 - k_3) \end{bmatrix} \begin{bmatrix} i_d \\ i_q \end{bmatrix} \qquad (12)$$

Arbitrary current sharing between winding sets requires two additional current controller pairs, one for each x-y plane. Since (12) provides d-q current references, current control should be implemented in an appropriate rotational reference frame. Direction of rotation is given in (11), where d-q current complex conjugate governs anti-synchronous rotation.

The previous analysis dealt with an asymmetrical nine-phase machine with three isolated neutral points. The configuration with a single neutral point is addressed next, in

which case the machine will be represented with three *x-y* planes and a single zero sequence. The applied VSD transformation matrix is as follows [22]:

$$[T_{9a1}] = \frac{2}{9} \begin{bmatrix} \cos([\theta_a]) \\ \sin([\theta_a]) \\ \cos(5[\theta_a]) \\ \sin(5[\theta_a]) \\ \cos(7[\theta_a]) \\ \sin(7[\theta_a]) \\ \cos(3[\theta_a]) \\ \sin(3[\theta_a]) \\ \frac{1}{2}\cos(9[\theta_a]) \end{bmatrix} \quad (13)$$

Since VSD transformation for the first three subspaces (α-β, x_1-y_1, x_2-y_2) is the same as in (2), the developed current sharing technique holds true also in the case of the machine with a single neutral point. Nevertheless, analysis for the additional subspace and single zero-sequence component is still required. By multiplying phase currents in (5) with VSD matrix (13), the x_3-y_3 and zero-sequence currents are:

$$i_{x3} = \frac{1}{3}(2i_{z1} + i_{z2} - i_{z3}), \quad i_{y3} = \frac{\sqrt{3}}{3}(i_{z2} + i_{z3}) \quad (14a)$$

$$i_z = \frac{1}{3}(i_{z1} - i_{z2} + i_{z3}) \quad (14b)$$

The x_3-y_3 and zero sequence currents do not have any influence on the power sharing, since they govern relationships between common mode currents of winding sets. To reduce losses, these currents should be set to zero by not exciting the x_3-y_3 subspace and zero sequence.

In order to complete the analysis for the nine-phase case, a symmetrical machine is considered next. The phase propagation angles in this case are:

$$[\theta_s] = \begin{bmatrix} 0 & \frac{2\pi}{9} & \frac{4\pi}{9} & \frac{6\pi}{9} & \frac{8\pi}{9} & \frac{10\pi}{9} & \frac{12\pi}{9} & \frac{14\pi}{9} & \frac{16\pi}{9} \end{bmatrix} \quad (15)$$

Multiple three-phase Clarke's transformation remains as in (4) and symmetrical nine-phase VSD transformations for three and single neutral points are [12]:

$$[T_{9s3}] = \frac{2}{9} \begin{bmatrix} \cos([\theta_s]) \\ \sin([\theta_s]) \\ \cos(2[\theta_s]) \\ \sin(2[\theta_s]) \\ \cos(4[\theta_s]) \\ \sin(4[\theta_s]) \\ \frac{3}{2}\ 0\ 0\ \frac{3}{2}\ 0\ 0\ \frac{3}{2}\ 0\ 0 \\ 0\ \frac{3}{2}\ 0\ 0\ \frac{3}{2}\ 0\ 0\ \frac{3}{2}\ 0 \\ 0\ 0\ \frac{3}{2}\ 0\ 0\ \frac{3}{2}\ 0\ 0\ \frac{3}{2} \end{bmatrix} \quad (16)$$

$$[T_{9s1}] = \frac{2}{9} \begin{bmatrix} \cos([\theta_s]) \\ \sin([\theta_s]) \\ \cos(2[\theta_s]) \\ \sin(2[\theta_s]) \\ \cos(4[\theta_s]) \\ \sin(4[\theta_s]) \\ \cos(3[\theta_s]) \\ \sin(3[\theta_s]) \\ \frac{1}{2}\cos(9[\theta_s]) \end{bmatrix} \quad (17)$$
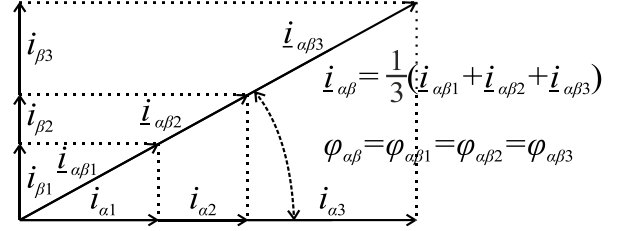

Fig. 3. Current vectors of all α–β planes. All individual winding set current vectors are aligned along the same axis in order to minimise the amplitude needed to sum up to $i_{\alpha\beta}$.

It should be noted that, instead of (17), one could use (13) for a symmetrical machine. However, such a transformation selection would lead to a different current component correlation, given with (6) for an asymmetrical nine-phase machine. Selecting the transformation matrices as in (17) (and hence (16) as well) for a symmetrical nine-phase machine keeps (6) valid for all cases, as discussed next.

When the previous analysis is repeated for a symmetrical machine, using equations (15), (4), (16), (17), the resulting set of equations is the same as (6)-(12). However, x_3-y_3 and zero-sequence equations in the case of a symmetrical machine with single neutral point differ from the asymmetrical case, and are given with:

$$i_{x3} = \frac{1}{3}(2i_{z1} - i_{z2} - i_{z3}), \quad i_{y3} = \frac{\sqrt{3}}{3}(i_{z2} - i_{z3})$$
$$i_z = \frac{1}{3}(i_{z1} + i_{z2} + i_{z3}) \quad (18)$$

As in the asymmetrical case, components in (18) do not have influence on power sharing. They represent common mode currents and should be kept at zero to reduce losses.

Provided that VSD transformations (2), (13), (16), (17) are used for machine model's decoupling, the analysis shows that (6) and (8) can be used for arbitrary power sharing among winding sets in all possible configurations of a nine-phase machine. Furthermore, when resistive loss minimisation criterion is applied, (12) is also applicable to all four machine topologies.

III. EXTENSION TO HIGHER PHASE NUMBERS

The previous analysis and the power sharing principle can be extended to any multiple three-phase winding machine. The starting point are again multiple three-phase Clarke's (4) and VSD transformations. The corresponding VSD transformation matrix can be obtained for any phase number using one of the available approaches for symmetrical or asymmetrical machines [11, 21-25]. In a general case an *n*-phase machine has *l* winding sets and *k* phases per winding set. Number of winding sets *l* can be any integer larger than 1, while *k* is the prime number, taken here as 3.

To adapt the VSD matrix to the power sharing algorithm, the rows are arranged as follows. The first pair is the one governing flux/torque producing subspace. The following pairs of rows for *x-y* subspaces are arranged for an asymmetrical machine from top to bottom in such a way that the order of the lowest odd non-triplen harmonic that maps into the subspace always increases as one moves downwards.

The matrix is completed with the triplen harmonic subspace(s) and/or zero-sequence homopolar component(s). In the case of a symmetrical machine the general transformation of [11] applies and it is only necessary to move the triplen harmonic subspace(s) towards the bottom, just above zero-sequence component(s). When this approach is applied to the nine-phase case, VSD transformations (2), (13), (16), (17) are obtained.

Procedure for obtaining relation between individual winding set and VSD currents is similar as in the nine-phase case. Namely, stator phase currents $[i_a, i_b, i_c, i_d, \dots]^T$ are obtained by use of inverse three-phase Clarke's transformation on α-β-z currents of each winding set. These phase currents are then multiplied by the VSD transformation matrix, resulting in the relationship between individual α-β-z winding set stator currents and VSD currents $[i_{\alpha\beta}, i_{xy1}, i_{xy2}, \dots, i_{z1}, i_{z2}, \dots]$. After some tedious algebraic manipulation, expressions that relate individual winding set currents and VSD currents are:

$$\underline{i}_{\alpha\beta} = \frac{1}{l}\sum_{i=1}^{l}\underline{i}_{\alpha\beta i}$$

$$\underline{i}_{xy_{ss}} = \begin{cases} \dfrac{1}{l}\sum_{i=1}^{l}\underline{\bar{i}}_{\alpha\beta i}\, e^{j3(ss+1)(i-1)\pi/n}, & ss=1,3,5,\dots \\ \dfrac{1}{l}\sum_{i=1}^{l}\underline{i}_{\alpha\beta i}\, e^{j3ss(i-1)\pi/n}, & ss=2,4,6,\dots \end{cases} \qquad (19)$$

Indices ss and i denote x-y subspace number and winding set number respectively. The second expression in (19) provides correlation between individual winding set currents ($\underline{i}_{\alpha\beta(1,2,\dots l)}$) and currents in the VSD subspaces ($\underline{i}_{\alpha\beta}$, $\underline{i}_{xy(1,2,\dots l-1)}$); thus, arbitrary control of generated/drawn power in each of the winding sets can be achieved by imposing currents in x-y planes. Depending on the parity of the subspace number (index ss), a different expression for x-y current is obtained.

The first expression in (19) shows that one l-th of the sum of all winding set currents ($\underline{i}_{\alpha\beta(1,2,\dots l)}$) is equal to the VSD total flux/torque producing current ($\underline{i}_{\alpha\beta}$). Consequently, ($l$-1) winding set currents can be controlled independently, while currents in one of the winding sets need to be governed by the existing power flow requirements. The rest of the x-y planes (triplen harmonic subspaces) and/or homopolar components are omitted from equation (19). They show relation to winding set common mode currents i_{z1}, i_{z2}, … i_{zl} and do not affect power sharing.

Expressions (19) are identical for all possible configurations of a machine with the selected phase number (symmetrical/asymmetrical with single/multiple neutral points). Moreover, (19) is based only on finding the relationship between VSD and the multiple three-phase Clarke's transformation. Hence, (19) is valid for any ac machine with multiple three-phase windings.

If minimal resistive loss criterion is introduced again, all α-β current vectors are aligned along the same axis ($\varphi_{\alpha\beta} = \varphi_{\alpha\beta 1} = \varphi_{\alpha\beta 2} = \dots = \varphi_{\alpha\beta l}$). Next, current sharing coefficients are introduced as ratio between amplitudes of individual winding set currents and amplitude of the total VSD flux/torque producing currents, as $k_i = I_{\alpha\beta i}/I_{\alpha\beta}$, $i=1, 2, \dots, l$. Equation (19) then becomes:

$$\sum_{i=1}^{l} k_i = l$$

$$\underline{i}^{*}_{xy_{ss}} = \begin{cases} \dfrac{1}{l}\sum_{i=1}^{l}k_i\, e^{j3(ss+1)(i-1)\pi/n}\underline{\bar{i}}_{\alpha\beta}, & ss=1,3,5,\dots \\ \dfrac{1}{l}\sum_{i=1}^{l}k_i\, e^{j3ss(i-1)\pi/n}\underline{i}_{\alpha\beta}, & ss=2,4,6,\dots \end{cases} \qquad (20)$$

The first expression in (20) shows that sum of the current sharing coefficient should be always equal to the number of the winding sets l. The second expression defines currents in complex form for the first (l-1) subspaces. Since the x-y currents are dependent only on the current sharing coefficients and the total flux/torque producing current, implementation of the current sharing is achieved by adding additional current control in the first (l-1) x-y subspaces.

Equations (20) are again valid for all multiphase machines with multiple three-phase winding sets, regardless of the actual machine configuration (symmetrical/asymmetrical with single or multiple neutral points). Hence the relationships (20) also apply to the case of an asymmetrical 12-phase machine with four neutral points, considered in [31, 32]. Clearly, if all current sharing coefficients k_i are equal to 1, x-y currents are equal to zero and the machine phase currents are balanced; power is shared equally between the three-phase winding sets.

To illustrate the theoretical considerations, numerical analysis is performed using Simulink. VSD transformation and current sharing have been created as described and as per (20), respectively, and different phase numbers are examined. Total flux/torque producing α-β currents with amplitude equal to 1 A and of 50 Hz fundamental frequency are supplied to the inverse VSD and current sharing blocks. Balanced operation is imposed in the beginning and at the end ($k_i = 1$, $i = 1, 2, \dots, l$), while in between current sharing coefficients are randomly varied to different values within the set $[1\dots l]$, with step changes taking place at 25 ms, 50 ms, 75 ms and 100 ms. The sum of the current sharing coefficients is always equal to the number of winding sets. Triplen harmonic subspace components and/or homopolar components are kept at zero value.

The analysis is performed for the six-, nine-, twelve- and fifteen-phase asymmetrical machines assuming a single neutral point (the same results are obtained with single and a multitude of isolated neutral points). Results can be seen in the Fig. 4 where α-β and x-y currents are shown in the left column, while phase currents are in the right column.

The current sharing coefficients are shown on the same plot with the corresponding winding set phase currents. Since α-β current amplitude is equal to 1 A, phase current amplitude is equal to the corresponding current sharing coefficient. The results confirm that arbitrary power/current sharing between winding sets is possible by imposing currents at the fundamental frequency in the x-y planes. Since total α-β currents are not affected, the flux and torque are unchanged.

The lower limit for current sharing coefficients is zero; however, upper limit is determined by current flux and torque requirements of the machine (i_d, i_q currents). Considering that currents in all winding sets should not exceed rated value, the following expression must hold true:

a) Six-phase case

b) Nine-phase case

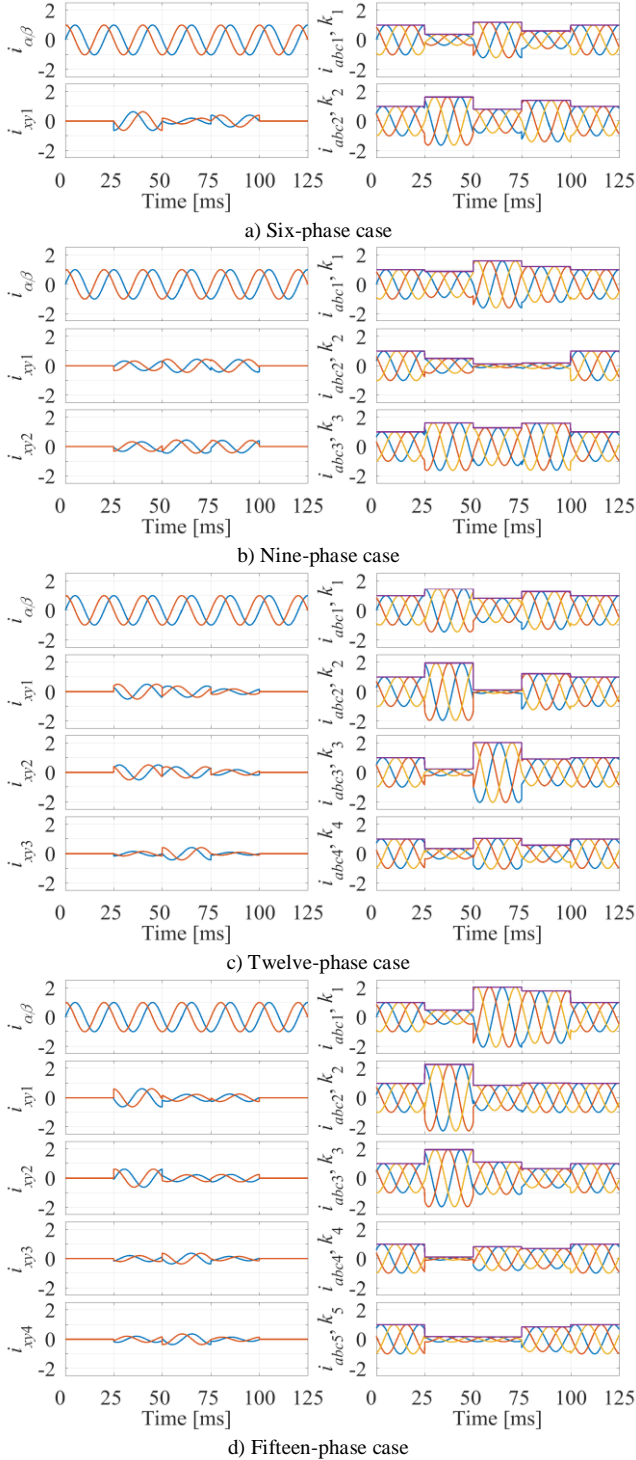c) Twelve-phase case

d) Fifteen-phase case

Fig. 4. Numerical results: Current sharing for six-, nine-, twelve- and fifteen-phase asymmetrical machine with a single neutral point.

$$0 \leq k_i \leq \frac{\sqrt{2}I_n}{\sqrt{i_\alpha^2 + i_\beta^2}}, \quad i = 1,2,3,\ldots,l \tag{21}$$

Unequal currents in individual winding sets lead to an unavoidable increase in the stator cooper losses. An analytical expression can be found by analysing copper losses in each winding set. Namely, if $I_{\alpha\beta i}$ is the amplitude of $\alpha\text{-}\beta$ current

vector in the ith winding set and amplitude invariant transformation is used, copper losses in said winding set are:

$$P_{\Omega s i} = \frac{3}{2}R_s I_{\alpha\beta i}^2 = \frac{3}{2}R_s k_i^2 I_{\alpha\beta}^2, \quad \left(I_{\alpha\beta i} = k_i I_{\alpha\beta}\right) \tag{22}$$

The total stator copper losses are then:

$$P_{\Omega s} = \frac{3}{2}R_s I_{\alpha\beta}^2 \sum_{i=1}^{l} k_i^2 \tag{23}$$

It is obvious that, when the machine is balanced, (23) provides well known expression for stator copper losses of a multiphase machine. On the other hand (23) is at maximum when only one (k_i^{th}) winding set is in operation ($k_i = l$). In this case stator copper losses are l times larger than in the balanced operation.

TABLE I. ASYMMETRICAL NINE-PHASE INDUCTION MACHINE PARAMETERS.

R_s	5.3 Ω	R_r	2.0 Ω
L_{ls}	24 mH	L_{lr}	11 mH
L_m	520 mH	P	1

IV. EXPERIMENTAL SET-UP AND CONTROL SCHEME

To verify theoretical considerations, an experimental set-up based on an asymmetrical nine-phase induction machine is used. The stator of a three-phase machine has been rewound to create an asymmetrical nine-phase winding. During the experiment, the machine is used as a generator in a configuration with three neutral points. The machine has 2 poles and is rated at 230 V and 2.2 kW. Parameters are listed in Table I. The shaft of the nine-phase machine is coupled to a dc machine by a Magtrol TM 210 torque meter. Torque meter has internal 2nd order analogue filter set to 200 Hz and its output is recorded by the oscilloscope. Dc machine is rated at 180 V, 3.7 kW, 1750 rpm and is supplied by a Sorensen SGI600/25 dc supply, which can operate in constant current mode. This enables constant torque operation of the dc machine.

The nine-phase machine is supplied using two custom-made inverters, based on Infineon FS50R12KE3 IGBT modules. The inverters have hardware-implemented dead time equal to 6 µs. Since the induction machine will work in generating mode, inverter dc link voltage (600 V) is provided by Spitzenberger & Spies linear amplifier PAS2500, which is capable of sinking power by use of accompanying resistive load RL4000. Measurement and control are realised by rapid prototyping platform dSPACE.

An ADC board is used to acquire phase currents measured by inverter's internal LEM sensors, while an incremental encoder board provides speed and position by capturing signals from an incremental encoder, mounted on the shaft of the nine-phase machine. Additional measurements are taken using Tektronix DPO/MSO 2014 oscilloscopes, equipped with current probes (TCP0030A) and high voltage differential probes (P5205A). Calculated winding set powers ($P_{wsj} = v_{aj}i_{aj} + v_{bj}i_{bj} + v_{cj}i_{cj}$, $j = 1, 2, 3$) were filtered by moving average filter with window width of 45 ms. Measured phase voltages, shown in the results, are filtered using a low-pass FIR filter, so that only the low frequency part of the spectrum, including

7

fundamental, is visible. The experimental set-up is shown in Fig. 5, while the corresponding schematic illustration is shown in Fig. 6. The configuration in effect corresponds to the stand-alone loading case of Fig. 1e, where the dc micro-grids are lumped into a single one. Overall phase voltage references are imposed using carrier-based PWM (CBPWM). The switching frequency is 5 kHz.

The machine control structure is based on the standard indirect rotor flux oriented control (IRFOC) [11]. Current control in the first subspace is performed in the rotor flux oriented (d-q) reference frame using PI controllers with cross-coupling decoupling (Fig. 7a). Voltage references for d-q axis voltage components are provided by the d-q current controllers. A PI controller is used in the speed control loop.

Fig. 5. Experimental set-up.
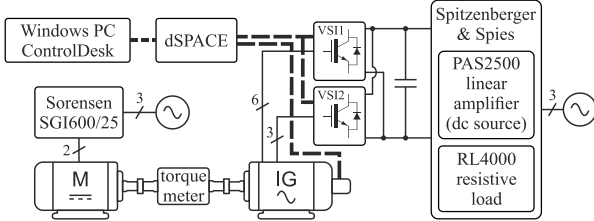
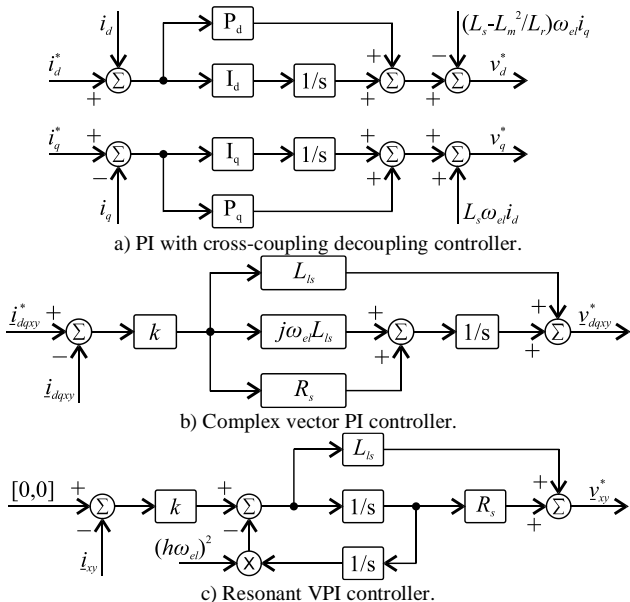Fig. 6. Schematic illustration of the experimental set-up.

a) PI with cross-coupling decoupling controller.

b) Complex vector PI controller.

c) Resonant VPI controller.

Fig. 7. Block diagrams of the used current controller structures (h denotes harmonic order).

Since flux/torque control is implemented in the d-q reference frame, current sharing control is also realised in the synchronous/anti-synchronous reference frames using (12). The inputs to the current sharing block are d-q current references ($i_d{}^*$, $i_q{}^*$), which are provided by the IRFOC block. As per (12), anti-synchronous and synchronous rotational transformations are used in x_1-y_1 and x_2-y_2 subspaces, respectively. It should be noted that current limit (21) is not implemented. Consequently, phase currents can rise above rated values, allowing for current sharing to be tested to the full extent. Current sharing coefficients can thus be changed in the range [0–3]. Complex vector PI regulators are implemented for current control in the x-y subspaces, as shown in Fig. 7b.

In addition to flux/torque and current sharing control, low-order harmonic elimination is also found to be necessary. Namely, +5th and +7th harmonics are present due to the inverter dead time, while -29th and -31st harmonics are present due to the non-ideal machine construction.

Harmonic elimination strategy by use of resonant controllers in synchronous reference frames, applicable to asymmetrical multiphase machines [29], has been adopted here. In this particular case, not all low-order harmonics are present. Consequently, resonant controllers and synchronous reference frames are tuned to different harmonic orders than the optimal ones proposed in [29]. Chosen resonant controllers are vector proportional integral (VPI), while harmonic orders to which synchronous reference frames and VPIs are tuned at are given in the Table II. To further reduce harmonic content of phase currents, eight different harmonics are eliminated in total, as per Table II. The VPI controller structure is shown in Fig. 7c.

The overall current control scheme consists of one PI pair in the d-q reference frame, two pairs of complex vector PIs (one in anti-synchronous x_1-y_1 and the other in synchronous x_2-y_2 frame) for current sharing control, and four resonant VPIs (two in each x-y plane for low order harmonics elimination). The low-order harmonic control (4 resonant current controllers) does not impact on current sharing. Schematic of the complete control system is given in Fig. 8.

V. EXPERIMENTAL RESULTS

The power sharing capabilities are tested while the nine-phase machine is used as an induction generator. The dc machine works in constant torque mode, while the nine-phase machine keeps the speed at the set value. Rotational speed is set to 1250 rpm and prime mover torque is set to -7 Nm. The current sharing coefficients are set according to the following sequence:

- [0.0 – 0.2] s - k_1=1, k_2=1, k_3=1;
- [0.2 – 0.6] s - k_1=0.4, k_2=1.2, k_3=1.4;
- [0.6 – 1.0] s - k_1=0.7, k_2=1.8, k_3=0.5;
- [1.0 – 1.4] s - k_1=1.5, k_2=0, k_3=1.5;
- [1.4 – 1.8] s - k_1=0, k_2=3, k_3=0;
- [1.8 – 2.0] s - k_1=1, k_2=1, k_3=1.

In the beginning and at the end of the experiment (0.2 s intervals) the machine is balanced and the current sharing

coefficients are equal to 1. The first two unbalanced sequences (0.4 s intervals) demonstrate the ability to arbitrarily control the phase current amplitudes in each winding set. The subsequent coefficient variations consider a case when one or two winding sets are completely switched off (0.4 s intervals). As a result, the machine operates as a six- or a three-phase one, respectively. This demonstrates one of the solutions for fault-tolerant operation, by switching off entire winding set.

Current sharing coefficients, VSD currents, and d-q currents of individual winding sets are shown in Fig. 9, while phase currents can be seen in the Fig. 10. Currents in x-y subspaces (the 3rd and 4th plot in Fig. 9) are governed by the current sharing coefficients (1st plot in Fig. 9) and instantaneous flux/torque producing d-q/α-β currents ($2^{nd}/5^{th}$ plot in Fig. 9), as per (12). Consequently, current sharing between winding sets is achieved according to the applied coefficients, as can be seen from the individual winding d-q current plots in Fig. 9 and phase currents shown in Fig. 10.

Currents in Fig. 9 are calculated from phase currents, which are obtained using the inverter's internal LEM sensors. Since acquisition is happening just before the control loop is executed, in the beginning and in the middle of the switching period, acquired data represent currents averaged over one switching period. Hence, switching ripple cannot be captured. On the other hand, phase currents i_{a1}, i_{a2}, and i_{a3} are captured by the oscilloscope and they are shown in the Fig. 10 for the same operating sequence as in Fig. 9.

Machine's speed, measured torque and generated electrical powers (total and in individual winding sets) are shown in Fig. 11. It can be observed that power sharing between winding sets corresponds to the coefficient values. A noticeable drop in the total extracted power is due to the increased stator winding losses, as per (23). The machine under test here is a low power one, with a relatively large stator resistance; hence the increase in copper losses and drop in extracted power, which is especially severe when only one three-phase winding is operational. The last plot in Fig. 11 shows that there is no substantial increase in the phase voltages during the current/power sharing. Therefore, an increase in dc link voltage would not be required during implementation of the proposed current/power sharing technique.

TABLE II. CONFIGURATION OF IMPLEMENTED RESONANT CONTROLLERS.

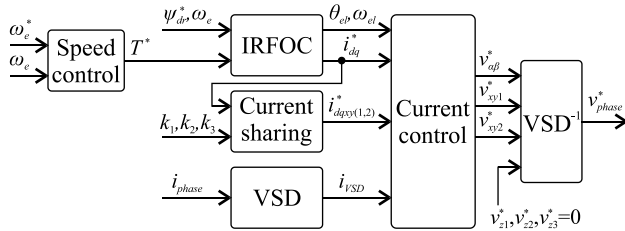| Resonant Controller	Subspace	Rotation	Harmonic order	Controlled harmonics
VPI 1	x_1-y_1	-4	9	+5 / -13
VPI 2			27	+23 / -31
VPI 3	x_2-y_2	-2	9	+7 / -11
VPI 4			27	+25 / -29

Fig. 8. The complete control system structure.

The change in the winding set currents/powers does not have any impact on the flux/torque producing α-β currents. Hence, average torque and speed are unaffected. Even more importantly, phase currents within one winding set are always kept balanced.

The previous experiment shows current sharing in steady state operation. The same experiment is performed next during the speed transient. The machine is accelerated from 1000 rpm to 1500 rpm within the 2 seconds time period. The measured torque is now -6 Nm, with acceleration torque of 1 Nm (hence the prime mover torque stays at -7 Nm, as in the steady state test). The same sets of results as for the steady state are shown in Figs. 12–14. It can be seen that developed current/power sharing technique is also valid during the speed transient and flux and torque producing d-q/α-β currents are not affected by applied current sharing between winding sets. Once again, phase currents i_{a1}, i_{a2}, and i_{a3}, shown in Fig. 13, are recorded by the oscilloscope. Since machine is now accelerating, while the torque is unchanged, extracted powers (Fig. 14) are changing during the experiment run. It should be noted that, in both experimental runs, a brief change in torque during the activation/ deactivation of one or two winding sets is evident and it is the result of a sudden change in machine operation and finite current controllers' bandwidth.

A decrease in the extracted power during the current/power sharing, caused by an increase in the stator copper losses according to (23), is obvious in Figs. 11 and 14. Fig. 15 shows stator winding losses obtained using measured phase currents ($P_{\Omega m} = \Sigma R_s i_j^2$, $j = 1, 2 \dots 9$) and using (23) ($P_{\Omega s}$) for the constant speed operation of Figs. 9-11. A good agreement between the two values is evident, thus confirming the validity of (23).

An increase in the torque ripple during the deactivation of one or two winding sets, which is evident in Fig. 11, is expected and it is the result of machine working as a six- or a three-phase one. Stator winding of the machine is of single-layer type [25], so that only one third of the slots is used in the mode when a single three-phase winding is operational.

VI. CONCLUSION

The possibility of arbitrary current/power sharing between three-phase winding sets of a multiphase machine has been addressed in this paper. Flux and average torque are unaffected and currents within each of the sets are balanced. The concept has been developed for all four topologies of a nine-phase machine, symmetrical/asymmetrical with one/ three neutral points. Arbitrary current/power sharing is obtained by imposing x-y currents of fundamental frequency. The principle is further expanded to cover all multiphase machines with multiple three-phase winding sets and the obtained equations are valid for any configuration (asymmetrical/symmetrical with one/multiple neutral points). An experimental set-up, with an asymmetrical nine-phase induction machine with three neutral points, has been used to confirm theoretical considerations. The machine has been driven as a generator in both constant and transient speed modes. The obtained experimental data show that arbitrary
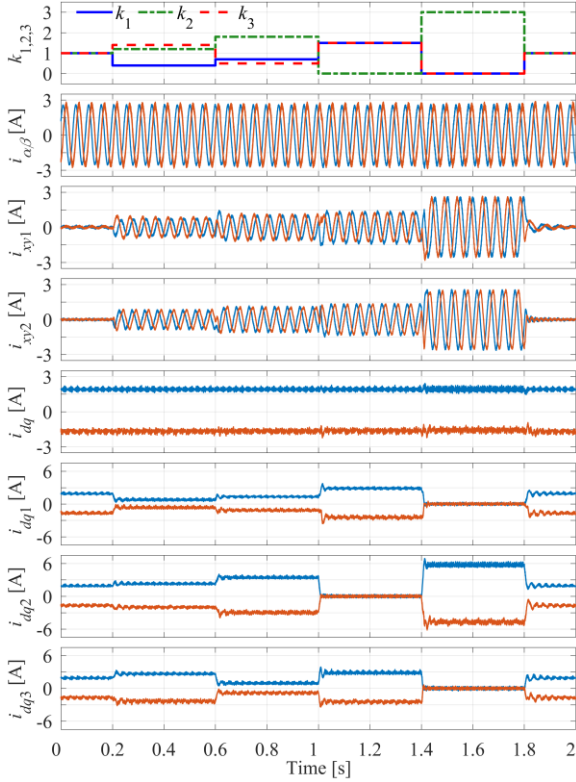
Fig. 9. Experimental results: Current sharing coefficients, VSD currents and winding set d-q currents during steady-state operation.
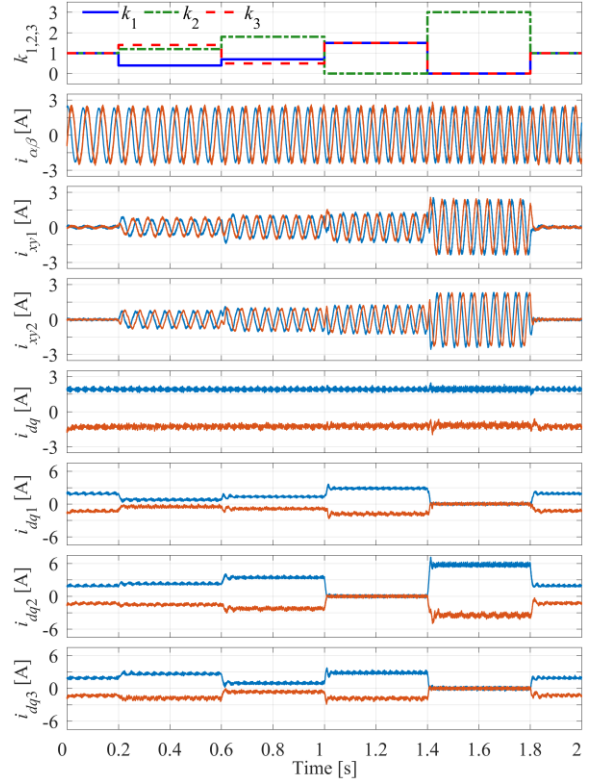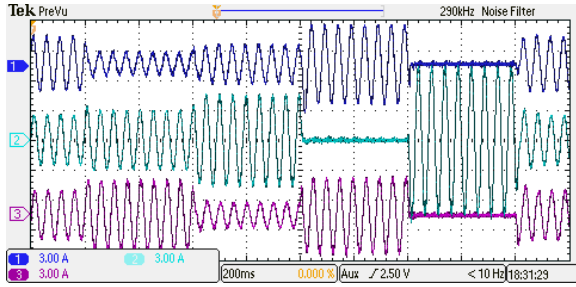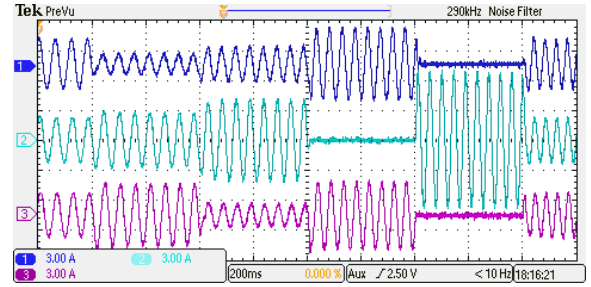

Fig. 10. Oscilloscope screenshot of the phase currents i_{a1}, i_{a2}, and i_{a3} during steady-state operation.
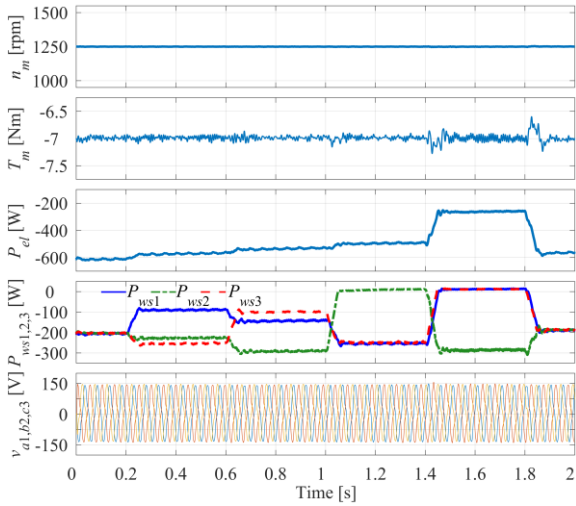

Fig. 11. Machine's speed, measured torque, electrical powers (total and winding sets) and phase voltages (v_{a1}, v_{b2}, v_{c3}) during steady state operation.

Fig. 12. Experimental results: Current sharing coefficients, VSD currents and winding set d-q currents during the speed transient.

Fig. 13. Oscilloscope screenshot of the phase currents i_{a1}, i_{a2}, and i_{a3} during the speed transient.
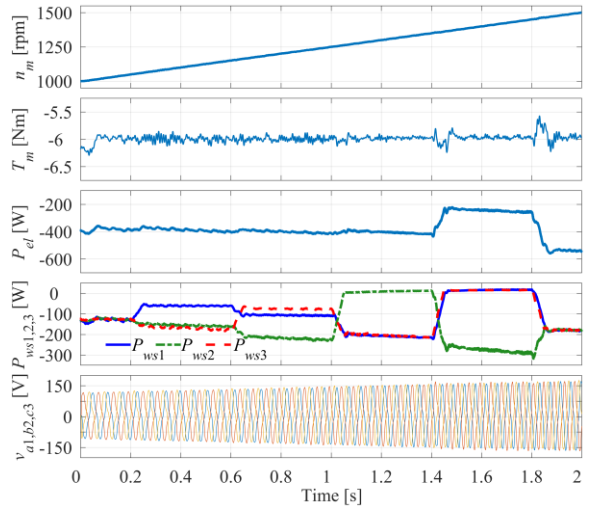

Fig. 14. Machine's speed, measured torque, electrical powers (total and winding sets) and phase voltages (v_{a1}, v_{b2}, v_{c3}) during the speed transient.
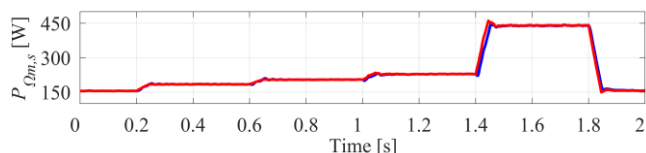
Fig. 15. Stator winding losses $P_{\Omega m}$ (blue) and $P_{\Omega s}$ (red) for the fixed speed operation at 1250 rpm.

current/power sharing between winding sets leads to an increase in the stator winding losses, which is also explained theoretically.

REFERENCES

[1] REN21, "Renewables 2016: Global status report (GSR)," *available at* *www.ren21.net*. Date accessed [14/12/2016].

[2] Siemens AG, "Siemens expands portfolio with 8 MW offshore wind turbine," *available at* *www.siemens.com/press/PR2016070338WPEN*. Date accessed [14/12/2016].

[3] MHI vestas offshore wind, "The V164-8.0 MW Turbine," *available at* *http://www.mhivestasoffshore.com/innovations/*. Date accessed [14/12/2016].

[4] K. Ma, L. Tutelea, I. Boldea, D. M. Ionel, and F. Blaabjerg, "Power electronic drives, controls, and electric generators for large wind turbines – an overview," *Electr. Power Comp. and Syst.*, vol. 43, no. 12, pp. 1406 - 1421, 2015.

[5] D. Vizireanu, S. Brisset, X. Kestelyn, P. Brochet, Y. Milet, and D. Laloy, "Investigation on multi-star structures for large power direct-drive wind generator," *Electr. Power Comp. and Syst.*, vol. 35, no. 2, pp. 135 - 152, 2007.

[6] J. Wang, R. Qu, and Y. Liu, "Comparison study of superconducting generators with multiphase armature windings for large-scale direct-drive wind turbines," *IEEE Trans. Applied Supercond.*, vol. 23, no. 3, Article sequence no. 5201005, 2013.

[7] K. Nounou, K. Marouani, M. Benbouzid, and B. Tabbache, "Six-phase induction machine operating as a standalone self-excited induction generator," in *Proc. IEEE Int. Conf. on Green Energy ICGEEEE*, Sfax, Tunisia, pp. 158 - 163, 2014.

[8] I. Gonzalez-Prieto, M. J. Duran, H. S. Che, E. Levi, M. Bermúdez and F. Barrero, "Fault-Tolerant operation of six-phase energy conversion systems with parallel machine-side converters," *IEEE Trans. on Power Electron*. vol. 31, no. 4, pp. 3068-3079, 2016.

[9] Z. Xiang-Jun, Y. Yongbing, Z. Hongtao, L. Ying, F. Luguang, and Y. Xu, "Modelling and control of a multi-phase permanent magnet synchronous generator and efficient hybrid 3L-converters for large direct-drive wind turbines," *IET Electr. Power Appl.,* vol. 6, no. 6, pp. 322 - 331, 2012.

[10] F. Wu, C. Tong, Y. Sui, L. Cheng and P. Zheng, "Influence of third harmonic back EMF on modeling and remediation of winding short circuit in a multiphase PM machine with FSCWs," *IEEE Trans. Ind. Electron.*, vol. 63, no. 10, pp. 6031-6041, 2016.

[11] E. Levi, R. Bojoi, F. Profumo, H. A. Toliyat, and S. Williamson, "Multiphase induction motor drives - a technology status review," *IET Electr. Power Appl.,* vol. 1, no. 4, pp. 489 - 516, 2007.

[12] E. Levi, "Multiphase electric machines for variable-speed applications," *IEEE Trans. Ind. Electron.,* vol. 55, no. 5, pp. 1893 - 1909, 2008.

[13] E. A. Klingshirn, "High phase order induction motors – part I: Description and theoretical considerations," *IEEE Trans. Power Appar. and Syst.,* vol. PAS-102, no. 1, pp. 47 - 53, 1983.

[14] F. Barrero and M. J. Duran, "Recent advances in the design, modeling, and control of multiphase machines – part I," *IEEE Trans. Ind. Electron.,* vol. 63, no. 1, pp. 449 - 458, 2016.

[15] M. J. Duran and F. Barrero, "Recent advances in the design, modeling, and control of multiphase machines – part II," *IEEE Trans. Ind. Electron.,* vol. 63, no. 1, pp. 459 - 468, 2016.

[16] E. Levi, "Advances in converter control and innovative exploitation of additional degrees of freedom for multiphase machines," *IEEE Trans. Ind. Electron.,* vol. 63, no. 1, pp. 433 - 448, 2016.

[17] R. H. Nelson and P. C. Krause, "Induction machine analysis for arbitrary displacement between multiple winding sets," *IEEE Trans. Power Appar. and Syst.,* vol. PAS-93, no. 3, pp. 841 - 848, 1974.

[18] G. K. Singh, K. Nam and S. K. Lim, "A simple indirect field-oriented control scheme for multiphase induction machine," *IEEE Trans. Ind. Electron.,* vol. 52, no. 4, pp. 1177-1184, 2005.

[19] E. Jung, H. Yoo, S. K. Sul, H. S. Choi and Y. Y. Choi, "A nine-phase permanent-magnet motor drive system for an ultrahigh-speed elevator," *IEEE Trans. Ind. Appl.*, vol. 48, no. 3, pp. 987-995, 2012.

[20] L. De Camillis, M. Matuonto, A. Monti, and A. Vignati, "Optimizing current control performance in double winding asynchronous motors in large power inverter drives," *IEEE Trans. Power Electron.,* vol. 16, no. 5, pp. 676 - 685, 2001.

[21] Y. Zhao and T. A. Lipo, "Space vector PWM control of dual three-phase induction machine using vector space decomposition," *IEEE Trans. Ind. Appl.,* vol. 31, no. 5, pp. 1100 - 1109, 1995.

[22] A. A. Rockhill and T. A. Lipo, "A simplified model of a nine phase synchronous machine using vector space decomposition," *Electric Power Components and Systems,* vol. 38, no. 4, pp. 477-489, 2010.

[23] M. A. Abbas, R. Christen, and T. M. Jahns, "Six-phase voltage source inverter driven induction motor," *IEEE Trans. Ind. Appl.,* vol. IA-20, no. 5, pp. 1251 - 1259, 1984.

[24] A. Tessarolo, "On the modeling of poly-phase electric machines through vector-space decomposition: theoretical considerations," in *Proc. IEEE Int. Conf. Power Eng., Energy and Electr. Drives POWERENG,* Lisbon, Portugal, pp. 519 - 523, 2009.

[25] I. Subotic, N. Bodo, E. Levi and M. Jones, "On-board integrated battery charger for EVs using an asymmetrical nine-phase machine," *IEEE Trans. Ind. Electron.*, vol. 62, no. 5, pp. 3285 - 3295, 2015.

[26] H. S. Che, E. Levi, M. Jones, W. P. Hew, and N. A. Rahim, "Current control methods for an asymmetrical six-phase induction motor drive," *IEEE Trans. Power Electron.*, vol. 29, no. 1, pp. 407 - 417, 2014.

[27] Y. Hu, Z. Q. Zhu, and K. Liu, "Current control for dual three-phase permanent magnet synchronous motors accounting for current unbalance and harmonics," *IEEE J. of Emerging and Selected Topics in Power Electron.,* vol. 2, no. 2, pp. 272 - 284, 2014.

[28] A. G. Yepes, J. Malvar, A. Vidal, O. López and J. Doval-Gandoy, "Current harmonics compensation based on multiresonant control in synchronous frames for symmetrical n -phase machines," *IEEE Trans. Ind. Electron.*, vol. 62, no. 5, pp. 2708-2720, 2015.

[29] A. G. Yepes, J. Doval-Gandoy, F. Baneira, D. Pérez-Estévez and O. López, "Current harmonic compensation for n-phase machines with asymmetrical winding arrangement", in *Proc. IEEE Energy Conv. Congress and Expo. ECCE*, Milwaukee, WI, pp. 1 - 8, 2016.

[30] S. Rubino, R. Bojoi, A. Cavagnino, and S. Vaschetto, "Asymmetrical twelve-phase induction starter/generator for more electric engine aircraft," in *Proc. IEEE Energy Conv. Congress and Expo. ECCE,* Milwaukee, WI, USA, cd-rom (EC-0902), 2016.

[31] A. Tani, G. Serra, M. Mengoni, L. Zarri, G. Rini, and D. Casadei, "Dynamic stator current sharing in quadruple three-phase induction motor drives," in *Proc. IEEE Annual Conf. of the Ind. Electron. Soc. IECON*, Vienna, Austia, pp. 5173-5178, 2013.

[32] M. Mengoni, G. Sala, L. Zarri, A. Tani, G. Serra, Y. Gritli, and M. Duran, "Control of a fault-tolerant quadruple three-phase induction machine for more electric aircrafts," in *Proc. IEEE Annual Conf. of the Ind. Electron. Soc. IECON,* Firenze, Italy, pp. 5747 - 5753, 2016.

[33] H. S. Che, E. Levi, M. Jones, M. J. Duran, W. P. Hew, and N. A. Rahim, "Operation of a six-phase induction machine using series-connected machine-side converters," *IEEE Trans. Ind. Electron.,* vol. 61, no. 1, pp. 164 - 176, 2014.

[34] M. Zabaleta, E. Levi, and M. Jones, "Modelling approaches for triple three-phase permanent magnet machines," in *Proc. Int. Conf. Electr. Mach. ICEM,* Lausanne, Switzerland, pp. 466-472, 2016.

Ivan Zoric (S'17) received the BSc and MSc degrees in Electrical Engineering from the University of Belgrade, Serbia in 2010 and 2013, respectively. Since June 2014 he is with Liverpool John Moores University, UK, where he is working towards a PhD degree. His main research interests include power electronics and advanced machine drives.

Martin Jones received his BEng degree (First Class Honours) in Electrical Engineering from the Liverpool John Moores University, UK in 2001. He was a research student at the Liverpool John Moores University from September 2001 till Spring 2005, when he received his PhD degree in Electrical Engineering. Dr Jones was a recipient of the IEE Robinson Research Scholarship for his PhD studies and is currently with Liverpool John Moores University as a Reader. His research is in the area of high performance ac drives.

Emil Levi (S'89, M'92, SM'99, F'09) received his MSc and the PhD degrees in Electrical Engineering from the University of Belgrade, Yugoslavia in 1986 and 1990, respectively. He joined Liverpool John Moores University, UK in May 1992 and is since September 2000 Professor of Electric Machines and Drives. He served as a Co-Editor-in-Chief of the IEEE Trans. on Industrial Electronics in the 2009-2013 period and is currently Editor-in-Chief of the IET Electric Power Applications and an Editor of the IEEE Trans. on Energy Conversion. He is the recipient of the Cyril Veinott award of the IEEE Power and Energy Society for 2009 and the Best Paper award of the IEEE Trans. on Industrial Electronics for 2008. In 2014 he received the "Outstanding Achievement Award" from the European Power Electronics (EPE) Association.